



Frequency locking in a nonlinear MEMS oscillator driven by harmonic force and time delay

Jerzy Warminski

Received: 4 August 2014 / Revised: 20 January 2015 / Accepted: 27 January 2015 / Published online: 11 February 2015
© The Author(s) 2015. This article is published with open access at Springerlink.com

Abstract Vibrations of a nonlinear self- and parametrically excited MEMS device driven by external excitation and time delay inputs are analysed in the paper. The model of MEMS resonator includes a nonlinear van der Pol function producing self-excitation, a periodically varied coefficient which represents Mathieu type of parametric excitation and furthermore, periodic force acting on the resonator. Analysis of frequency locking zones is presented with suggestions for a strategy of a closed loop control. Interactions between self- and parametric excitation lead to quasi-periodic oscillations but under specific conditions the motion becomes harmonic. The so called frequency locking, near the resonance zones is observed. This is caused by the second kind Hopf bifurcation (Neimark–Sacker bifurcation). The amplitudes of periodic oscillations are determined analytically by the multiple time scale method (MS) in the second order perturbation. The effect of external force has been observed by the internal loop occurring inside the frequency locking zone. The localisation of the zones and existence of the internal loop can be controlled by a selection of gains and time delay of displacement or velocity feedbacks.

Keywords Hopf bifurcations · Quasi-periodic oscillations · Frequency locking zones · Self-excitation · Parametric vibrations · Time delay · Control

1 Introduction

Many mechanical macro, micro or nano-scale devices have to be studied as nonlinear structures in order to explain

properly their dynamics. Micro–Electro–Mechanical Systems (MEMS) can be used as specific resonators designed in order to work as amplifiers, sensors, filters or nonlinear mixers. They can also be applied in various kind of scanning probe microscopes. As an example we can mention papers [1–3], or [4, 5] where MEMS devices are used as radio frequency resonators. In such MEMS devices different vibration modes may interact in the same time.

Reduced (simplified) models of MEMS devices are often proposed to reduce more accurate but computationally expensive models. Such approach is essential if the nonlinear resonator has to work in a complex network. A MEMS device designed as thin planar radio frequency resonator is presented in papers [4, 6]. The nonlinear dynamics of the MEMS is described by a one degree of freedom system modelled by Mathieu–van der Pol–Duffing ordinary differential equation with additional periodic force. It has been shown that the system can exhibit quasi-periodic motion or frequency locking either harmonic 1:1 or subharmonic 2:1. Analytical results obtained by the method of multiple scales have been compared with experimental tests for entrainment in a continuous wave (CW) laser driven limit cycle disc resonator. Recently, Duffing–van der Pol model has also been used for mathematical description of nonlinear dynamics of simply supported Si beams of 200 nm thick and 35 μm long [7]. The device self-oscillated in its first bending mode. Due to compressive prestress the micro-beam buckled, leading to a strong amplitude frequency dependence. Regions of the primary and secondary resonances have been measured experimentally and on this basis a reduced one degree of freedom model has been created. Limit cycle micro-oscillators have been studied in [8, 9]. A ten parameter theoretical model has been fit with experimental results. Apart from mechanical also a thermodynamical model has been adopted in order to couple average temperature to a nonlinear displacement field. The temper-

J. Warminski (✉)
Department of Applied Mechanics, Lublin University of Technology,
Nadbystrzycka 36, 20-618 Lublin, Poland
e-mail: j.warminski@pollub.pl

ature effect on MEMS beams dynamics has been discussed recently in [10, 11].

The mentioned above MEMS models include interacting three different modes of vibrations: self-, parametric and external excitation. Specific phenomena which may occur while all of them interact in the same time have been presented in [12, 13]. It has been demonstrated that the interaction between parametric and self-excitation leads to the secondary Hopf bifurcation and frequency locking zones. The studied models took into account self-excitation defined by nonlinear Rayleigh or van der Pol functions and parametric excitation by time varying coefficients. The influence of external force has been demonstrated for one degree of freedom (DOF) [12–14] and for a two DOF [15] system. It has been shown there that small external force may qualitatively change vibrations near the principal parametric resonance. The added force affected the resonance curve by the internal loop occurrence. The loop phenomenon was also studied in [16] for a two degrees of freedom system in a contents of a nonlinear normal modes formulation. A study of quasi-periodic oscillations driven by parametric and external excitations have been presented in [17–19]. Apart from suppression of the primary and subharmonic resonances also analysis of an existence of quasi-periodic vibrations and suppression of chaotic motion have been presented there.

The secondary Hopf bifurcation and frequency quenching near parametric resonances for various type of damping models have been analysed in [20–25]. Parametric resonances and Hopf bifurcations in a harmonic oscillator with nonlinear damping and elasticity with application to MEMS device consisting of 30 μm diameter silicon disk have been presented in [26]. In [27] perturbation analysis of quasi-periodic Mathieu equation have been studied in order to determine the size of instability regions.

It is worth mentioning that the mathematical models applied to MEMS devices have important meaning in macro structures as well. In papers [28, 29] wind-induced vibrations of a tower system have been presented. A model of the structure with self-excited vibrations, interacting with external or/and parametric excitations confirmed results published in [16].

Time delays may occur in the model as inputs of a natural process or can be considered as control signals artificially imposed to the system in order to control its dynamics. A control strategy for a self-excited Rayleigh type system driven by parametric and external excitation by adding a time delay signal has been presented in paper [30]. The effect of time delay on nonlinear oscillations near the resonance zones has been shown there. The added displacement feedback has been proposed to control the system response. A harmonically forced Duffing oscillator with time delay have been studied in [31] and recently in [32]. By using the method of multiple scales the resonances have been derived and the

concept of an equivalent damping related to the delay feedback has been proposed. Dynamics of a delayed nonlinear Mathieu equation with cubic nonlinearity, near 2:1 parametric resonance has been presented in [33]. It has been shown that the instability region can be eliminated for sufficiently large delay gains and appropriately chosen time delay. Control of van der pol-Duffing oscillator under time delayed position and velocity feedbacks has also been studied in [34] by perturbation method. The effective control of vibration amplitude has been possible if time delay and feedback gains have been chosen properly.

This paper is a continuation of the study of a self- and parametrically excited system presented in [30] where Rayleigh–Mathieu–Duffing model was analysed with influence of external force and displacement feedback. In this paper we consider van-der Pol–Mathieu–Duffing model corresponding to MEMS devices discussed above in the literature review. The van der Pol damping is taken into account as a term which can produce self-excitation. This is a phenomenological approach which is used to describe specific dynamics of selected MEMS or NEMS resonators. The limit cycle oscillations occur in micro beams, disks or dome shaped systems. Driving these devices by using either a piezoactuator or a modulated laser at certain energy level the devices may spontaneously transit into limit cycle oscillations. The sign of damping may become negative, making unstable the equilibrium position and leading to self-excited oscillations represented by a limit cycle. This phenomenon can be well represented by van der Pol model of damping [7, 8, 10, 11]. Furthermore, we consider an effect of external force, displacement and velocity feedbacks in order to control the MEMS device.

2 Model

The MEMS resonator is modelled by a one degree of freedom (DOF) oscillator, composed of nonlinear spring with cubic nonlinearity and a damper with nonlinear van der Pol damping. The assumed nonlinear damping may produce self-excitation as a stable limit cycle with an unstable equilibrium point inside. A periodically varied in time coefficient represents parametric excitation of Mathieu type. Furthermore the system can be excited externally by external harmonic force.

The mathematical model of the MEMS resonator is formulated on the basis of papers [4, 6]. The considered Mathieu–van der Pol–Duffing model is a phenomenological reduction of a real MEMS device. In spite of the fact that the structure is simple, just with one degree of freedom, its dynamics may be complex. Interactions between three different vibrations: self-, parametric and external, may lead to specific phenomena. Dynamics of such a MEMS resonator may be controlled by adding external harmonic force (open loop control) or time delay function taken from response of the system

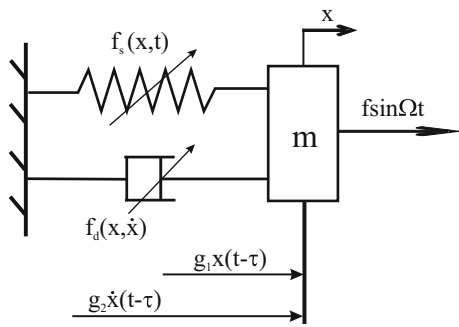


Fig. 1 Nonlinear model of a self-, parametric and externally excited system with time delay signal

(closed loop control). In this paper we focus on the influence of external force on MEMS dynamics and furthermore we study the effect of two delayed inputs, displacement and velocity delay. A physical model of the MEMS resonator is presented in Fig. 1.

The dynamics of the resonator is governed by the nonlinear ordinary differential equation:

$$\ddot{x} + (-\alpha + \beta x^2) \dot{x} + (1 - \mu \cos 2\Omega t) x + \gamma x^3 = f \cos \Omega t + g_1 x(t - t_d) + g_2 \dot{x}(t - t_d). \quad (1)$$

Equation (1) includes: van der Pol term of self-excitation represented by parameters \$\alpha\$ and \$\beta\$, Mathieu parametric term with amplitude \$\mu\$ and frequency \$2\Omega\$, cubic Duffing nonlinearity with \$\gamma\$ coefficient. On the right hand side, there are: external harmonic force with amplitude \$f\$ and frequency \$\Omega\$ and two feedbacks considered as displacement and velocity control signals with time delay \$t_d\$ and gains \$g_1\$ and \$g_2\$. Equation (1) has a very general form. It allows an analysis of interesting singular cases by switching on–off selected terms. We note that external force excites the system in 1 : 2 ratio with respect to parametric excitation. It means that near the principal parametric resonance the system is excited parametrically with frequency \$2\Omega\$ while its response is subharmonic with frequency \$\Omega\$. Thus, the external force excites the system additionally with frequency equal to the response.

Equation (1) can be solved numerically. The numerical solution is close to the strict one. But in such approach the qualitative analysis and parameters influence is limited. The model based control strategy is also difficult to realise. Therefore in this paper the system is solved analytically with the direct numerical simulation used for results validation.

The system is nonlinear thus we apply an approximate method in order to get analytical solution. Following the paper [30] where the Rayleigh model of self-excitation was analysed, in similar way we apply the multiple time scale method [35]. We derive the ‘slow flow’ in the second order perturbation and on this basis we find fixed points corresponding to periodic solutions of the original system. The slow-flow equations will allow also determining bifurca-

tion points of periodic into quasi-periodic solutions and then amplitudes of quasi-periodic oscillations (see [17, 18, 36]). In this paper however, we focus on the periodic oscillations and their bifurcation points close to the frequency locking zones.

3 Slow flow: periodic solutions

In order to study the systems dynamics, we solve Eq. (1) analytically by the multiple time scale method [35]. We assume that the system is weakly nonlinear. Thus the differential equation of motion is rewritten in the form

$$\ddot{x} + x = \varepsilon \left[(\tilde{\alpha} - \tilde{\beta}x^2) \dot{x} + x\tilde{\mu} \cos 2\Omega t - \tilde{\gamma}x^3 + \tilde{f} \cos \Omega t + \tilde{g}_1 x(t - t_d) + \tilde{g}_2 \dot{x}(t - t_d) \right] \quad (2)$$

where \$\varepsilon\$ is a formal small parameter, used for grouping ‘small’ terms on the right hand side of Eq. (2). Now, the parameters are defined as: \$\alpha = \varepsilon \tilde{\alpha}\$, \$\beta = \varepsilon \tilde{\beta}\$, \$\mu = \varepsilon \tilde{\mu}\$, \$\gamma = \varepsilon \tilde{\gamma}\$, \$f = \varepsilon \tilde{f}\$, \$g_1 = \varepsilon \tilde{g}_1\$, \$g_2 = \varepsilon \tilde{g}_2\$. In further notation however, ‘tilde’ is dropped for simplicity.

The whole procedure for obtaining the analytical solution is presented in “Appendix”. The approximate solutions are sought near the principal parametric resonance zone in the second perturbation order. According to the method we assume the solution in a series of a small parameter (18). We also introduce different scales of time (19). Around the principal parametric resonance, frequency of excitation \$\Omega\$ is expressed by the detuning parameter \$\sigma_1

$$\Omega^2 = \omega_0^2 + \varepsilon \sigma_1 \quad (3)$$

where, \$\omega_0\$ is natural frequency of a linear system and in our case \$\omega_0 = 1\$. Following the procedure given in “Appendix”, the solution takes the form

$$x(t) = a \cos(\Omega t + \phi) - \varepsilon \frac{a}{16\Omega^2} \left[\mu \cos(3\Omega t + \phi) - \frac{1}{2}\gamma a^2 \cos 3(\Omega t + \phi) + \frac{1}{2}a^2 \beta \Omega \sin 3(\Omega t + \phi) \right] \quad (4)$$

Amplitude \$a = a(t)\$ and phase \$\phi = \phi(t)\$ are time dependent functions and they are determined from modulation equations (slow flow)

$$\begin{aligned} 2\Omega a \frac{da}{dt} &= \varepsilon \left(\alpha \Omega a - \frac{1}{4}a^3 \beta \Omega - \frac{1}{2}a\mu \sin 2\phi - g_1 a \sin \tau \right. \\ &\quad \left. + g_2 \Omega a \cos \tau - f \sin \phi \right) \\ &+ \varepsilon^2 \left\{ -\frac{3}{8\Omega} a^3 \alpha \gamma + \frac{1}{16\Omega} \beta \gamma a^5 \right. \\ &\quad \left. - \frac{1}{2\Omega^2} g_1^2 a \cos \tau \sin \tau - \frac{1}{2} g_2^2 a \cos \tau \sin \tau \right. \\ &\quad \left. + f \left[\frac{1}{4\Omega} \left(-\alpha + \frac{1}{4}a^2 \beta \right) \cos 2\phi \right] \right\} \end{aligned}$$

$$\begin{aligned}
& + \frac{1}{4\Omega^2} \left(\frac{1}{2}\mu - \sigma_1 + \frac{9}{2}a^2 \right) \sin 2\phi \\
& + \frac{1}{32\Omega^2} a^3 \mu (\beta\Omega \cos 2\phi + 5\gamma \sin 2\phi) \Big] \\
& + g_1 \frac{1}{2\Omega^2} \left[a \left(-\sigma_1 + \frac{3}{2}\gamma a^2 \right. \right. \\
& \left. \left. - \frac{1}{2}\mu \cos 2\phi \right) \sin \tau - \frac{1}{2}f \sin(\phi + \tau) \right] \\
& + g_2 \left[\frac{1}{4\Omega} \left(-\frac{1}{2}\gamma a^3 \cos \tau - f \cos(\phi + \tau) \right) \right. \\
& \left. + \frac{1}{2} \left(-\alpha a + \frac{1}{4}\beta a^3 + \frac{1}{2\Omega} \mu a \sin 2\phi \right) \right] \Big\} \\
2\Omega a \frac{d\phi}{dt} = & \varepsilon \left(\frac{3}{4}a^3 \gamma - a\sigma_1 - \frac{1}{2}a\mu \cos 2\phi - g_1 a \cos \tau \right. \\
& - g_2 a\Omega \sin \tau - f \cos \phi) \\
& + \varepsilon^2 \left\{ -\frac{1}{4}a\alpha^2 + \frac{3}{32\Omega^2} a\mu^2 + \frac{3}{8\Omega^2} a^3 \gamma \sigma_1 \right. \\
& + \frac{1}{4}\alpha\beta a^3 - \frac{1}{4\Omega^2} a\sigma_1^2 \\
& - \frac{1}{128}a^5 (7\beta^2 + 15\gamma^2) - \frac{1}{4\Omega^2} g_1^2 a \cos 2\tau \\
& - \frac{1}{4}g_2^2 a \cos 2\tau - \frac{1}{16\Omega^2} \mu a^3 (\gamma \cos 2\phi \\
& + \beta\Omega \sin 2\phi) \\
& + f \left[\frac{1}{4\Omega^2} \left(\frac{1}{2}\mu - \sigma_1 + \frac{3}{4\Omega^2} a^2 \right) \cos \phi \right. \\
& \left. + \frac{1}{4\Omega} \left(\alpha - \frac{3}{4}\beta a^2 \right) \sin \phi \right] \\
& + g_1 \left[\frac{1}{2\Omega^2} a \left(\frac{3}{4}a^2 \gamma - \sigma_1 \right) \cos \tau \right. \\
& \left. - \frac{1}{8\Omega} \beta a^3 \sin \tau - \frac{1}{4\Omega^2} f \cos(\phi + \tau) \right. \\
& \left. + \frac{1}{8\Omega^2} a\mu (\cos(\tau - 2\phi) - \cos(\tau + 2\phi)) \right] \\
& + g_2 \left[\frac{1}{2}a \left(-\alpha + \frac{1}{4}\beta a^2 \right) \cos \tau \right. \\
& \left. + \frac{1}{4\Omega} f \sin(\phi + \tau) \right. \\
& \left. + \frac{1}{8\Omega} a\mu (\sin(\tau - 2\phi) + \sin(\tau + 2\phi)) \right] \Big\} \quad (5)
\end{aligned}$$

Parameter τ is time delay defined as: $\tau = \Omega t_d$. On the basis of the above slow flow equations we can study analytically amplitude and phase of vibrations and also the bifurcation points. Equations (5) are also used to study an influence of the most important parameters.

As we can notice the modulation equation in the second order perturbations have quite complex form, therefore we start the analysis from the first order approximation. Neglecting in Eq. (5) terms of ε^2 order, assuming a steady state

$$\begin{aligned}
\frac{da}{dt} = 0, \frac{d\phi}{dt} = 0, \text{ we get} \\
a \left[\Omega \left(\alpha - \frac{1}{4}a^2 \beta \right) - \frac{1}{2}\mu \sin 2\phi - g_1 \sin \tau \right. \\
\left. + g_2 \Omega \cos \tau \right] = f \sin \phi \\
a \left(\frac{3}{4}a^2 \gamma - \sigma_1 - \frac{1}{2}\mu \cos 2\phi - g_1 \cos \tau \right. \\
\left. - g_2 \Omega \sin \tau \right) = f \cos \phi \quad (6)
\end{aligned}$$

Equations (6) describe amplitudes of periodic oscillations near the principal parametric resonance. The first order perturbation solution are less precise than those of the second order. But the advantage of using them is their simpler form, often giving possibility to be solved. The equations in the first order perturbation (6) can be used as a starting point for solving the second order problem (5).

In further numerical analysis, on the basis of papers [12–14, 30] we accept the values of parameters:

$$\begin{aligned}
\alpha = 0.01, \beta = 0.05, \gamma = 0.1, \mu = 0.2, \\
f \in (0, 0.5), g_1 \in (-1, 1), g_2 \in (-1, 1), \tau \in (-2\pi, 2\pi) \quad (7)
\end{aligned}$$

Selected parameters are varied in wide ranges in order to demonstrate specific dynamic phenomena.

4 Stability analysis

Stability of the solutions is determined on the basis of the first order perturbation. Taking into account terms of ε order, Eqs. (5) are rewritten in the shorter form

$$\begin{aligned}
\frac{da}{dt} = f_1(a, \phi) \\
\frac{d\phi}{dt} = f_2(a, \phi) \quad (8)
\end{aligned}$$

where

$$\begin{aligned}
f_1(a, \phi) = & \frac{1}{2\Omega a} \left(\alpha \Omega a - \frac{1}{4}a^3 \beta \Omega - \frac{1}{2}a\mu \sin 2\phi \right. \\
& \left. - g_1 a \sin \tau + g_2 \Omega a \cos \tau - f \sin \phi \right) \\
f_2(a, \phi) = & \frac{1}{2\Omega a} \left(\frac{3}{4}a^2 \gamma - a\sigma_1 - \frac{1}{2}a\mu \cos 2\phi \right. \\
& \left. - g_1 a \cos \tau - g_2 a\Omega \sin \tau - f \cos \phi \right) \quad (9)
\end{aligned}$$

To analyse stability of the steady-state solutions, Eqs. (8) are linearized with respect to a and ϕ and then the Jacobian matrix is defined

$$J = \begin{bmatrix} \frac{\partial f_1}{\partial a} & \frac{\partial f_1}{\partial \phi} \\ \frac{\partial f_2}{\partial a} & \frac{\partial f_2}{\partial \phi} \end{bmatrix} \quad (10)$$

The characteristic equation of the Jacobian (10) takes the form

$$\lambda^2 - Tr(J)\lambda + Det(J) = 0 \quad (11)$$

and phase

$$\tan 2\phi = \frac{4\alpha\Omega - a^2\beta\Omega + 4g_2\Omega \cos \tau - 4g_1 \sin \tau}{-3a^2\gamma + 4\sigma_1 + 4g_1 \cos \tau + 4g_2\Omega \sin \tau} \quad (15)$$

From Eq. (14) we find vibration amplitudes

$$a_{1,2} = \sqrt{\frac{1}{9\gamma^2 + \beta^2\Omega^2} \left\{ 4g_1(3\gamma \cos \tau - \beta\Omega \sin \tau) + 4g_2\Omega(3\gamma \sin \tau + \beta\Omega \cos \tau) + 6\gamma\sigma_1 + 2\alpha\beta\Omega^2 \right.} \\ \left. \pm \frac{1}{4}\sqrt{64[3\gamma\sigma_1 + \alpha\beta\Omega^2 + (3g_1\gamma + g_2\beta\Omega^2)\cos \tau - (g_1\beta - 3g_2\gamma)\Omega \sin \tau]^2 - 16(9\gamma^2 + \beta^2\Omega^2)} \right. \\ \left. \times [4g_1^2 - \mu^2 + 4\sigma_1^2 + 4g_2^2\Omega^2 + 8(g_1\sigma_1 + g_2\alpha\Omega^2)\cos \tau - 8(g_1\alpha - g_2\sigma_1)\Omega \sin \tau] \right\}} \quad (16)$$

where λ is an eigenvalue of the Jacobian matrix. The trace $Tr(J)$ and determinant $Det(J)$ are defined as:

$$Tr = \frac{1}{2}\alpha - \frac{3}{8}\beta a^2 + \frac{1}{4\Omega}\mu \sin 2\phi + \frac{1}{2\Omega}g_1 \sin \tau \\ + \frac{1}{2}g_2 \cos \tau + \frac{1}{2a\Omega}f \sin \phi \\ Det = \frac{\mu}{4\Omega} \left[\frac{3}{4\Omega}a^2\gamma \cos 2\phi + \left(\alpha - \frac{3}{4}a^2\beta \right) \sin 2\phi \right] \\ - \frac{\mu^2}{8\Omega^2} \sin^2 2\phi \\ + \frac{f}{4\Omega} \left[\frac{3}{4\Omega}a\gamma \cos \phi + \left(\frac{\alpha}{a} - \frac{1}{4}a\beta \right) \sin \phi \right. \\ \left. + \frac{\mu}{a\Omega} \left(\cos \phi \cos 2\phi - \frac{1}{2} \sin \phi \sin 2\phi \right) \right] \\ - \frac{g_1}{4\Omega^2} \left(\frac{f}{a} \sin \phi + \mu \sin 2\phi \right) \sin \tau \\ + \frac{g_2}{4\Omega} \left(\frac{f}{a} \cos \phi + \mu \sin 2\phi \right) \cos \tau + \frac{f^2}{4a^2\Omega^2} \cos^2 \phi \quad (12)$$

The solution is asymptotically stable if the roots of the characteristic equation have negative real parts. From the Routh-Hurwitz criterion, the solution of the system is stable if and only if

$$Tr(J) < 0 \text{ and } Det(J) > 0. \quad (13)$$

5 Parametric and self-excited system with time delay

Let us consider a case without external force. Substituting in Eq. (6) $f = 0$, after simple algebraic manipulations we get the equation for amplitude

$$\frac{1}{4}a^4(9\gamma^2 + \beta^2\Omega^2) + a^2 \left[\Omega(-2\alpha\beta\Omega^2 - 6\gamma\sigma_1) \right. \\ \left. + 2g_1(-3\sigma_1 \cos \tau + \beta\Omega \sin \tau) \right. \\ \left. - 2g_2\Omega(\beta\Omega \cos \tau + 3\gamma \sin \tau) \right] \\ + 4 \left(\sigma_1^2 + \alpha^2\omega^2 - \mu^2 + g_2^2\Omega^2 + g_1^2 \right) = 0 \quad (14)$$

Above amplitudes represent the region of a periodic solution which corresponds to frequency locking or frequency quenching zone [20–22, 24]. This phenomenon consists in quenching frequency of self-excited vibrations by parametric excitation [30]. Outside this region the motion is quasi-periodic, demonstrated by a limit cycle on Poincaré map or modulated oscillations in time domain. In the present analysis we will focus mainly on periodic response and frequency locking regions.

Amplitudes (16) depend on the structural parameters, and gains g_1 and g_2 and time delay τ of delayed signals. Selecting properly these three coefficients of input signals we can control the system's response. If we assume that g_1 and g_2 are equal to zero then we get dynamics of the system without the feedbacks. This state corresponds to a case without control. Next, we look for a possible dynamics modification by the delayed signals activation. The influence of the delayed signals we demonstrate by switching on-off selected gains g_1 or g_2 . The resonance curve without any feedbacks is presented in Fig. 2a. The black curve shows the response for $g_1 = 0$ and $g_2 = 0$ with solid and dashed line denoting stable and unstable solutions, respectively. We see that the resonance curve is located around $\Omega \approx 1$ with Hopf bifurcation point (HB) indicated on the left branch. Out of the frequency-locking zone quasi-periodic solutions exist. They bifurcate into the periodic solution in HB point located on the solid line. It means that adding the displacement feedback with gain g_1 and delay $\tau = 0$ we may shift the frequency locking zone with a minor change of the amplitude and the HB point localisation (Fig. 2a). However, varying time delay τ we may influence essentially the amplitudes with a minor shift of the curves. This is shown in Fig. 2b. The displacement feedback with $g_1 = 0.15$ and $\tau = -0.5$ increased amplitudes, moved the HB point and enlarged the unstable solution region. For positive values of time delay $\tau = 0.49$ amplitudes have been decreased and left branch of the curve stabilised.

The analytical results have been validated by direct numerical simulations of Eq. (2) by means of Runge–Kutta method

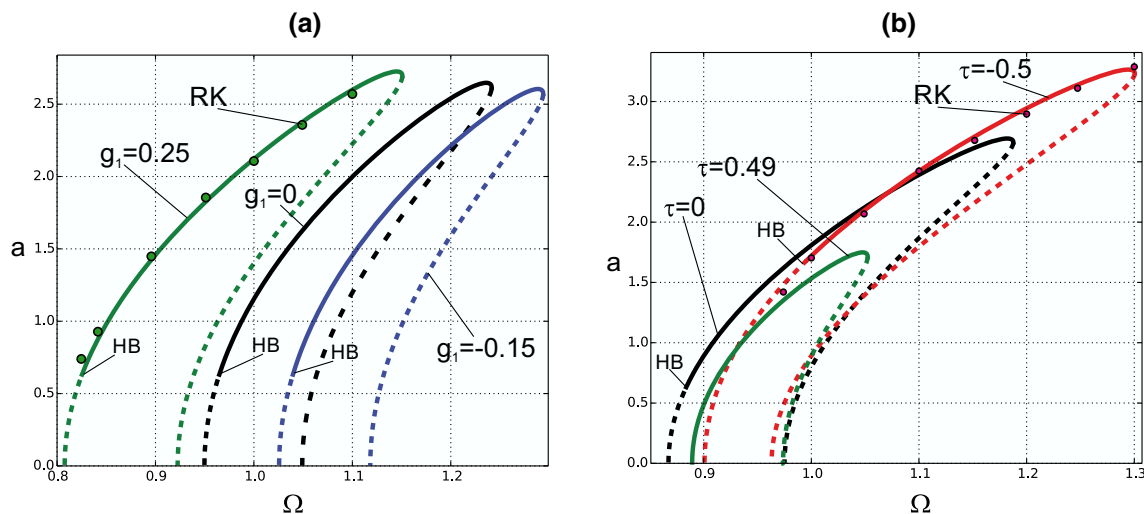


Fig. 2 Resonance curves **a** for $\tau = 0$ and selected values of gain $g_1 := (0.25, 0, -0.15)$, and **b** for $g_1 = 0.15$ and selected values of time delay $\tau := (-0.5, 0, 0.49)$; $f = 0, g_2 = 0$; HB—Hopf bifurcation point, RK—direct numerical simulation by Runge–Kutta method

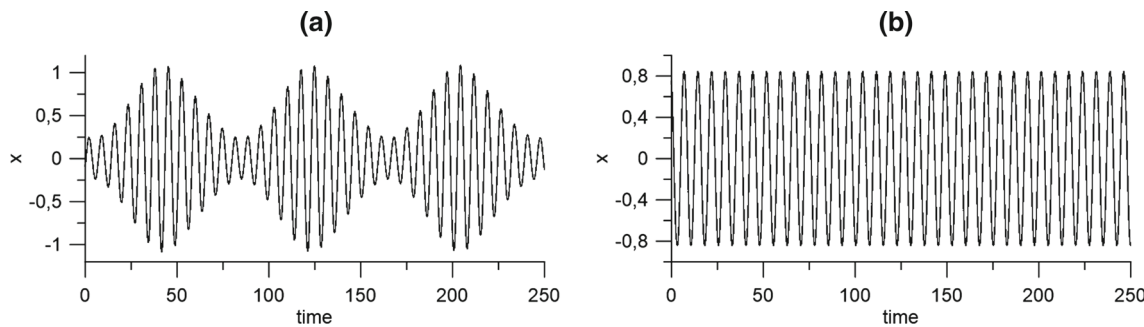


Fig. 3 Time histories for $\Omega = 0.83$ **a** and $\Omega = 0.84$ **b**; gain $g_1 = 0.25$, $\tau = 0$, $f = 0$, $g_2 = 0$ —numerical simulations

(RK) of the forth order. Obtained numerically amplitudes are marked by circles and denoted by RK in Fig. 2. For the curve $g_1 = 0.25$ and $\tau = 0$ (Fig. 2a) there is a very good agreement of the numerical and analytical results, as well as the prediction of the Hopf bifurcation point. Numerical solutions just before ($\Omega = 0.83$) and after the Hopf bifurcation point ($\Omega = 0.84$) are presented in Fig. 3a, b respectively. As predicted analytically, the quasi-periodic solution bifurcates into periodic one.

Another comparison has been done for $g_1 = 0.15$ and $\tau = -0.5$. In this case the analytical prediction of amplitudes again corresponds very well to numerical simulations (see circles in Fig. 2b). However, the prediction of the Hopf bifurcation differs in the sense that numerical results are stable in wider region then predicted analytically (see circles on the left, next to the HB point). This difference results from the accuracy of the analytical method. We have to consider this fact designing the control strategy close to the HB point. For $\Omega = 0.94$ we get quasi-periodic motion and for $\Omega = 0.95$ the solution tends to periodicity (Fig. 4).

We may want to act on the system response if the excitation frequency is fixed. Such a situation is presented in Fig. 5. The gain g_1 has an influence similar to the detuning parameter. The curve in Fig. 5a remains the resonance curve. Starting from zero value the increase or decrease of g_1 increases or decreases amplitudes respectively. The delay τ changes the amplitude in rather limited way (Fig. 5b) but it may cause instability in a relatively large region.

Similar analysis we perform for velocity feedback, assuming that $g_1 = 0$. The influence of gain g_2 is different than g_1 . Varying gain g_2 and keeping $\tau = 0$ we may influence amplitudes with almost no shift of the resonance curves (Fig. 6a). A shift of the resonance zone can be controlled by a proper selection of time delay τ which is demonstrated in Fig. 6b.

Analytical results are validated by bifurcation diagrams obtained from direct numerical simulation of Eq. (1). Diagrams in Fig. 7 correspond to the curves presented in Fig. 6a for $g_2 = 0.05$ and $g_2 = -0.05$. Solid line in Fig. 7a represents the frequency locking zone, black regions denote quasi-periodic oscillations. When we increase value of gain

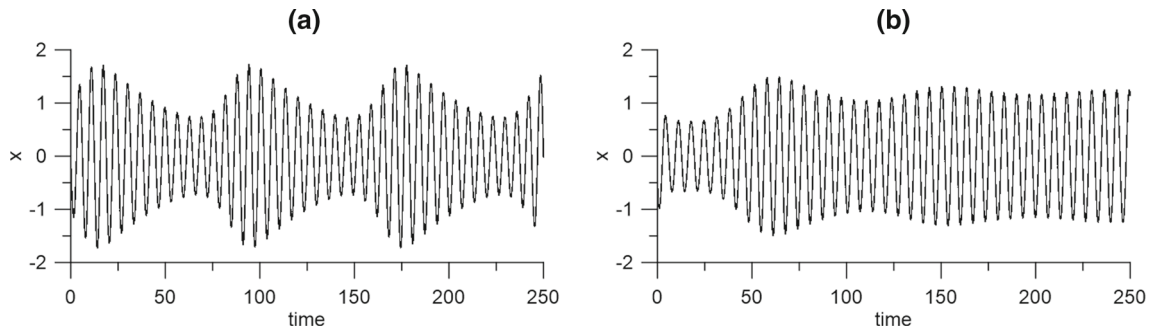


Fig. 4 Time histories for $\Omega = 0.94$ a and $\Omega = 0.95$ b; gain $g_1 = 0.15$, $\tau = -0.5$, $f = 0$, $g_2 = 0$ —numerical simulations

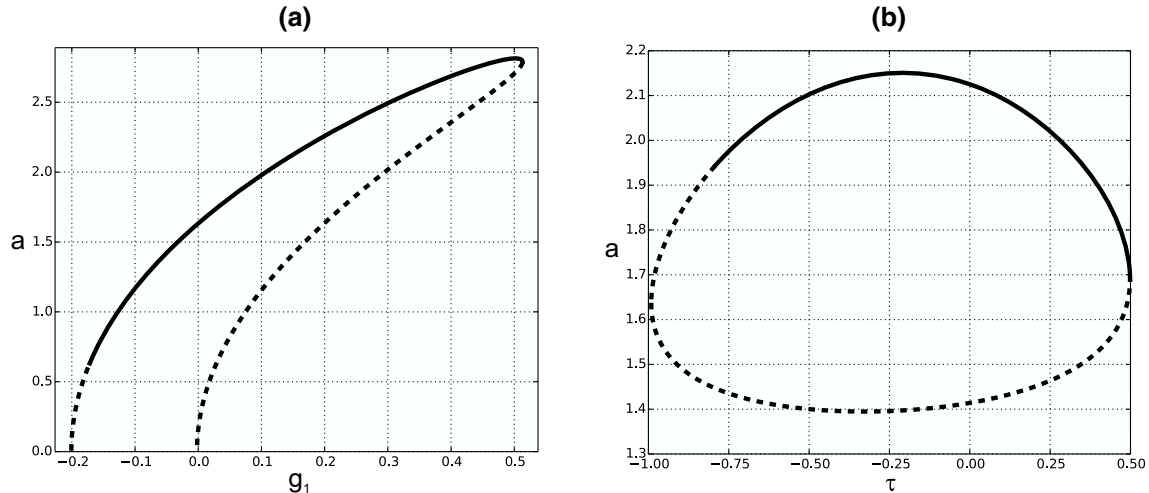


Fig. 5 Influence of displacement feedback for fixed excitation frequency $\Omega = 1.05$, a versus gain g_1 for $\tau = 0$ and b time delay τ for $g_1 = 0.15$; $f = 0$, $g_2 = 0$

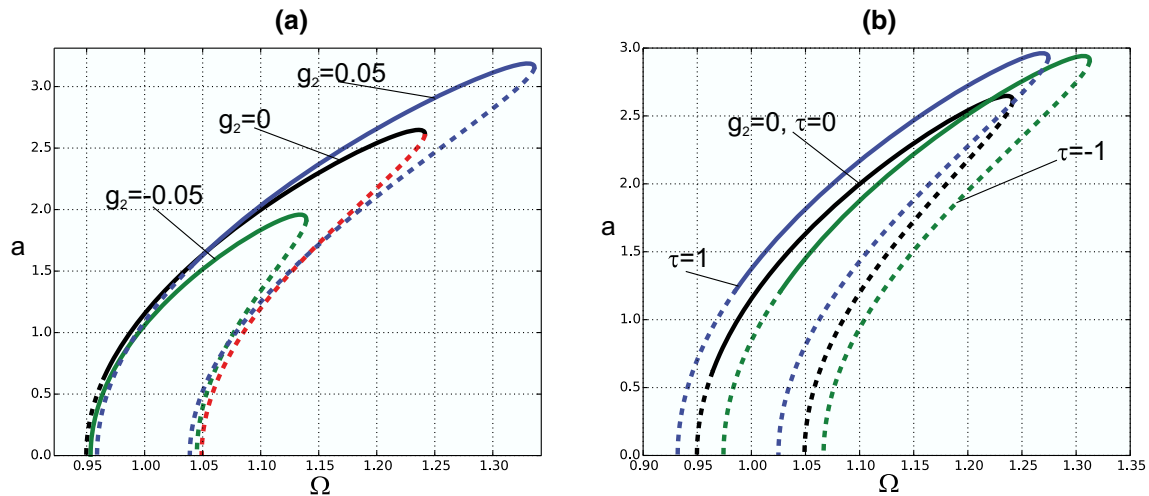


Fig. 6 Resonance curves for a $\tau = 0$ and selected values of gain $g_2 := (-0.05, 0, 0.05)$ and b for $g_2 = 0.05$ and time delay $\tau := (-1, 1)$ and $g_2 = 0, \tau = 0; g_1 = 0, f = 0$

g_2 then we can decrease amplitudes in the frequency locking zone and furthermore, eliminate quasi-periodicity (Fig. 7b). The effect of the velocity feedback is demonstrated also for

fixed excitation frequency Ω . We see that varying the gain g_2 we may influence amplitudes in a relatively small interval with the solutions in some intervals becoming unstable

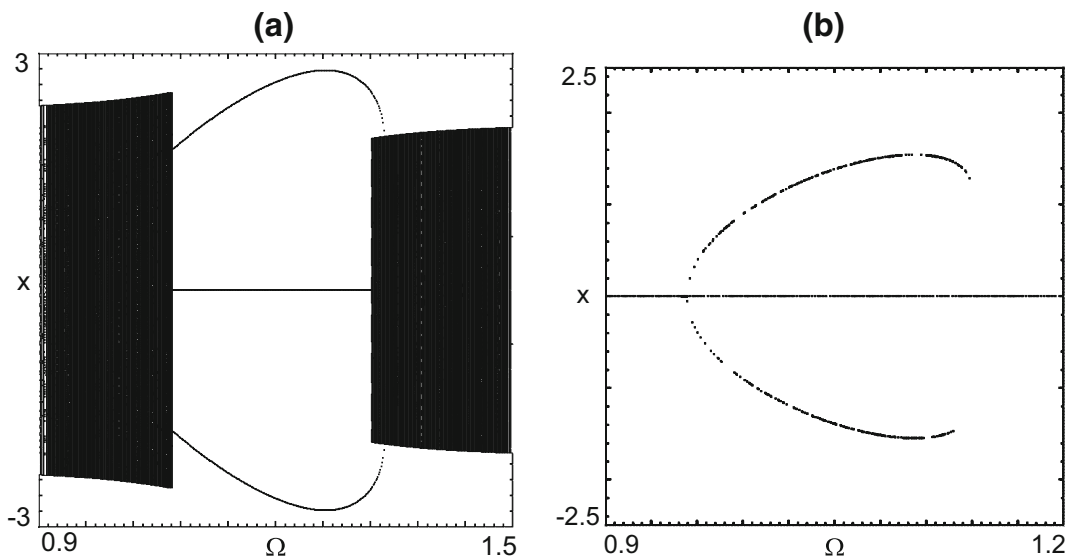


Fig. 7 Bifurcation diagrams for gain **a** $g_2 = 0.05, \tau = 0$ and **b** $g_2 = -0.05, \tau = 0; f = 0$

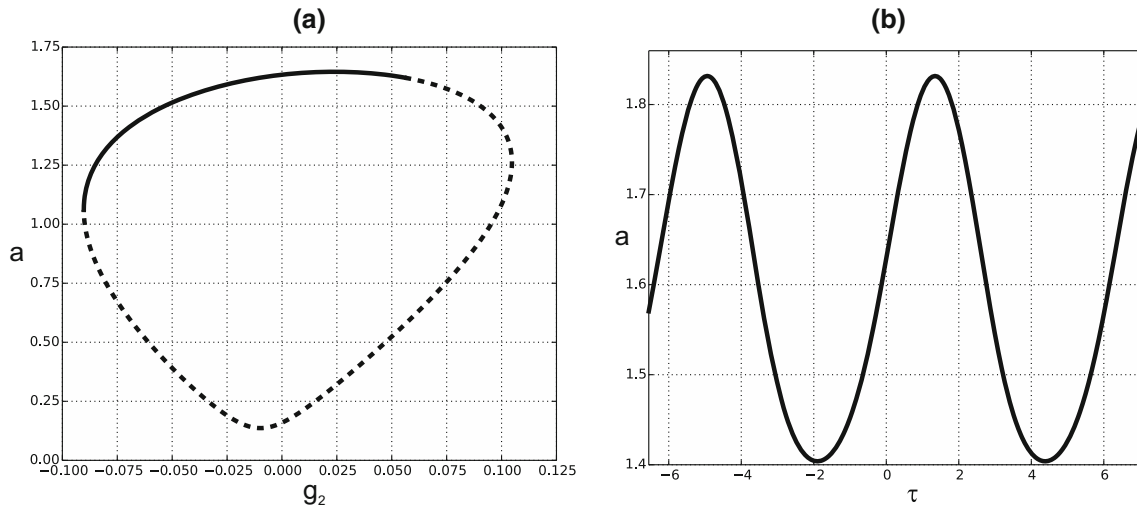


Fig. 8 Influence of velocity feedback for fixed excitation frequency $\Omega = 1.05$, **a** versus gain g_2 for $\tau = 0$ and **b** time delay τ for $g_2 = 0.05$; $f = 0, g_1 = 0$

(Fig. 8a). The variation of delay τ does not influence stability for the selected frequency but just changes the amplitude $a \in (1.4, 1.83)$.

Let assume that we are looking for gains values and time delay leading to amplitude reduction to zero $a = 0$. Equaling to zero Eq. (16) we find

$$g_2\Omega = \sqrt{\mu^2 - 4[g_1^2 - \sigma_1^2 - \alpha^2\Omega^2(-1 + \cos^2\tau) + 2g_1\alpha\Omega \sin\tau + \sigma_1^2 \sin^2\tau + 2\sigma_1 \cos\tau(-g_1 + \alpha\Omega \sin\tau)]} \quad (17)$$

Equation (17) allows determining gain g_2 for selected values of structural parameters, versus gain g_1 and time delay τ

for which amplitude of periodic oscillations is equal zero. In Fig. 9 we present gain g_2 as a function of frequency Ω for different values of gain g_1 and delay τ . We may observe that time delay τ turns left the solutions (Fig. 9b), gain g_1 shifts the solution left (Fig. 9c) and both g_1 and τ move the solution left and up (Fig. 9d).

The surfaces of gain g_2 against frequency Ω and gain g_1 as well as g_2 against frequency Ω and delay τ are presented

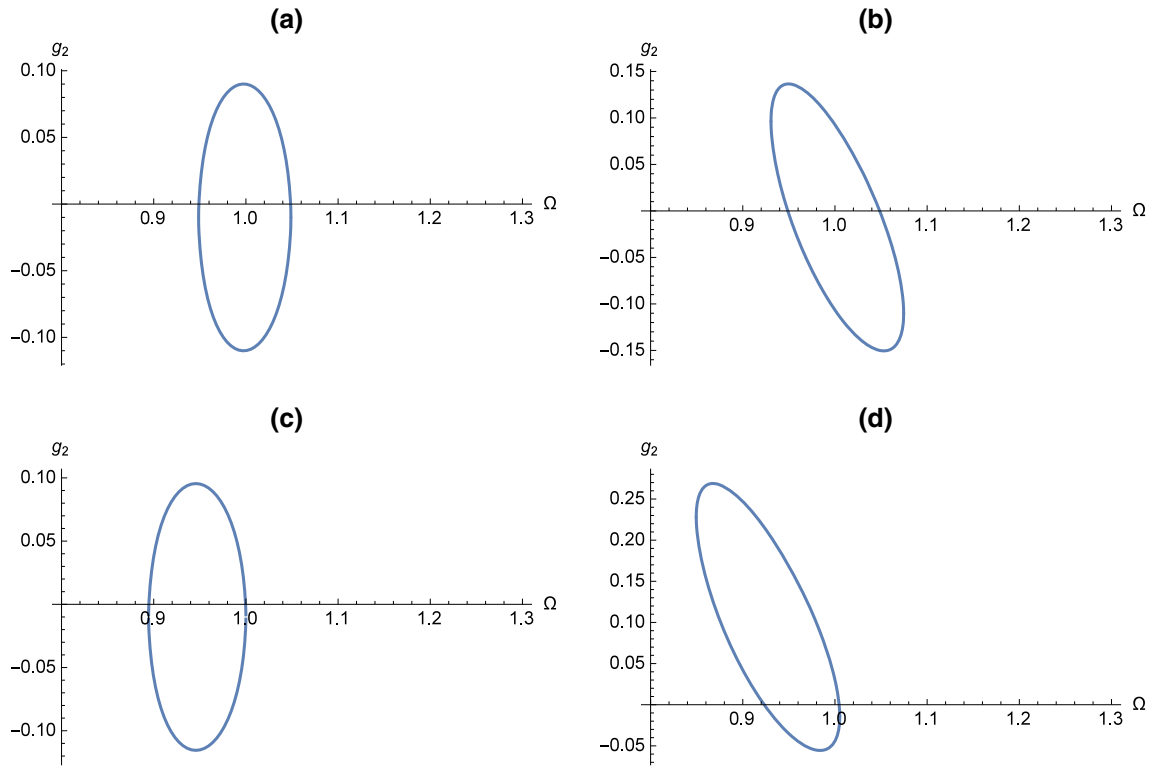
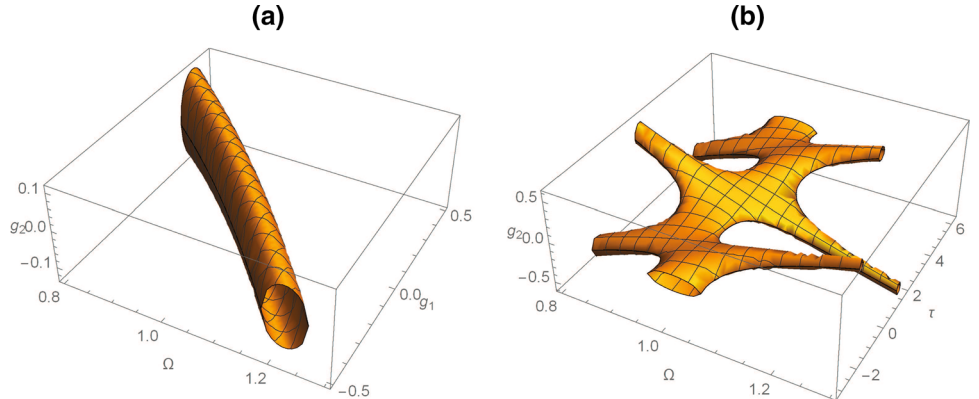


Fig. 9 Gain g_2 against frequency Ω computed from Eq. (17) for **a** $g_1 = 0$, $\tau = 0$, **b** $g_1 = 0$, $\tau = 0.8$, **c** $g_1 = 0.1$, $\tau = 0$, **d** $g_1 = 0.1$, $\tau = 0.8$; $f = 0$

Fig. 10 3D plots of gain g_2 against **a** frequency Ω and gain g_1 or **b** frequency Ω and time delay τ computed from Eq. (17) for **a** $\tau = 0$, **b** $g_1 = 0.05$; $f = 0$



in Fig. 10 in 3D plots. Curves presented in Fig. 9 are cross-sections of the 3D surfaces. In Fig. 10b we see periodicity with respect to time delay τ . On basis of 3D plots (Fig. 10) and their 2D cross-sections (Fig. 9) we can find values of the control parameters g_1 , g_2 and τ for which the amplitude is suppressed to zero.

6 Parametrically and self-excited system with external force and time delay

Let us consider the resonator which apart from self- and parametric excitation is forced by harmonic force. Frequency of external force is tuned 1:2 with respect to parametric excita-

tion. The model of the resonator with external force has been derived for MEMS device in papers [4, 6]. This kind of equation was studied before in [14]. Periodic, quasi-periodic and chaotic oscillations with detailed description of the bifurcation scenario were presented there. In this paper we focus on periodic oscillations and frequency locking zones, mainly.

In this section we study the slow flow dynamics described by Eq. (5) with imposed external force, displacement and velocity feedbacks. The steady state solutions we can find from the second order perturbation or we can simplify the problem to the first order Eq. (6). Because it has not been possible to solve analytically the set of nonlinear algebraic equations either in the second or the first perturbation order, therefore we decided to solve the modulation equations

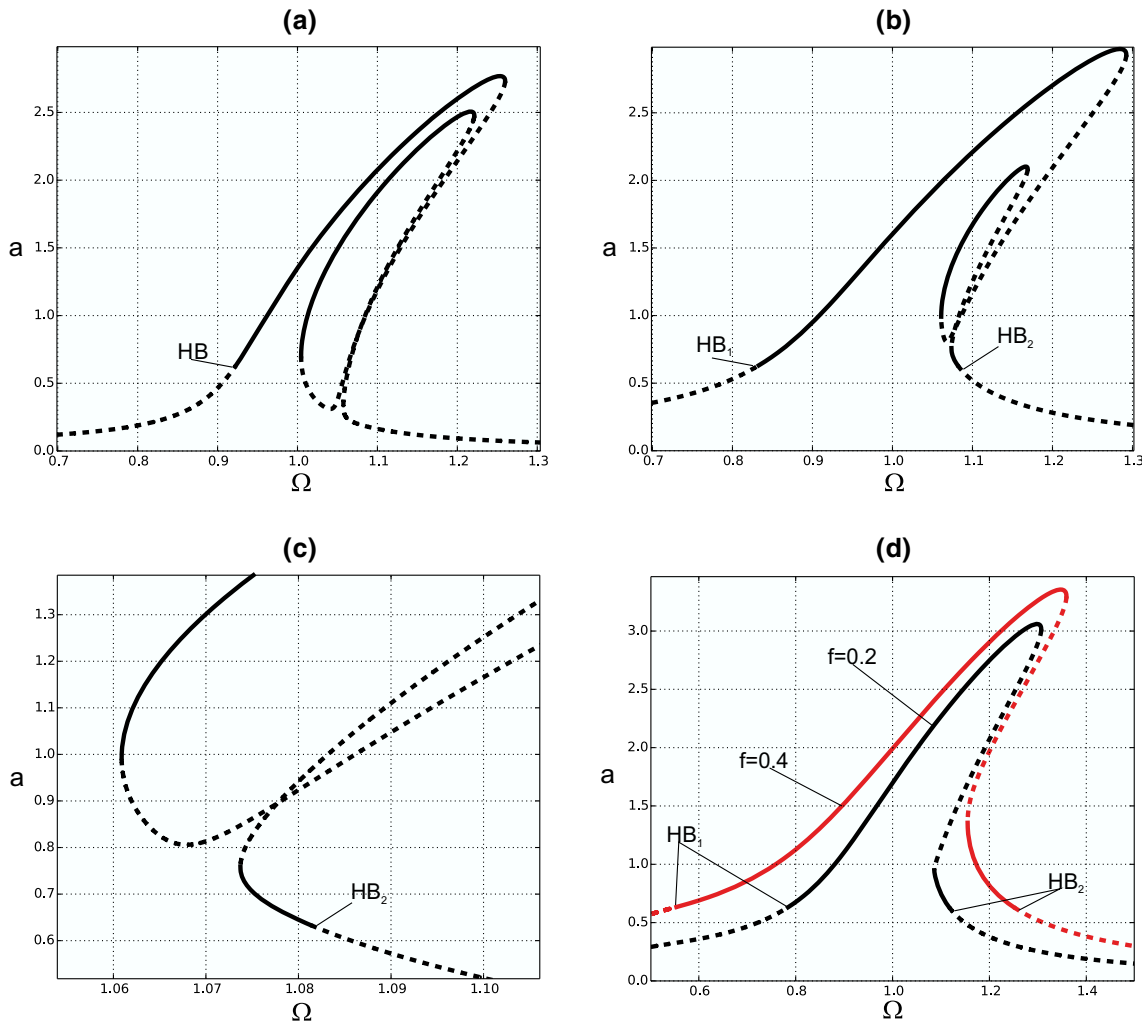


Fig. 11 Resonance curves for various values of external force **a** $f = 0.05$ **b** $f = 0.15$, **c** $f = 0.15$ —zoom around HB_2 , **d** $f = 0.2$ —black and $f = 0.4$ —red; $g_1 = 0$, $g_2 = 0$. (Color figure online)

numerically. The second order Eqs. (5) have been introduced to *Auto* package and then studied by the continuation method [37].

At first we consider the model without feedback influence, $g_1 = 0$, $g_2 = 0$. The added external harmonic force changed the response of the resonator. The frequency locking zone is qualitatively different. Small harmonic force caused appearance of the internal loop. The stability analysis shows that only upper branch of the internal loop is stable. We get five steady state solutions: two upper stable and three lower unstable (Fig. 11a). The loop diminishes when the external force increases (Fig. 11b) and finally, after a certain threshold it vanishes (Fig. 11d) and the resonance curve gets a classical shape. Another important phenomenon is the second kind of Hopf Bifurcation (HB) point (Neimark–Sacker bifurcation) in which quasi-periodic oscillations bifurcate into periodic. For small force there is only one HB point located on the left branch (Fig. 11a), for increased force apart from HB_1 also the second HB_2 occurs on the right branch (Fig. 11b, c,

d). The right branch, initially unstable, transforms into stable one, with HB_2 point. The zoom of the zone near HB_2 is presented in Fig. 11c.

The external force has important influence on the system dynamics. It may change the resonance curve course and a number of obtained solutions. In Fig. 12 we demonstrate influence of external force for fixed frequency $\Omega = 1.05$ (region with three solutions) and $\Omega = 1.1$ (region with five solutions). In fact, increasing external force above $f > 0.13$ or below $f < -0.13$ we move from triple solution to a single solution region (Fig. 12a). For $\Omega = 1.1$ the five solution region is located in $f \in (-0.2, 0.2)$. Increasing f for $0.2 < |f| < 0.24$ we get the triple solution region and above $|f| > 0.24$ the single stable solution (Fig. 12b).

In order to control system response we take the resonance curve for $f = 0.15$ (Fig. 12b) as a basic curve. Then we introduce displacement feedback. The response for fixed frequency $\Omega = 1.1$ and varied g_1 gain and time delay τ is presented in Fig. 13. The gain g_1 behaves similar to

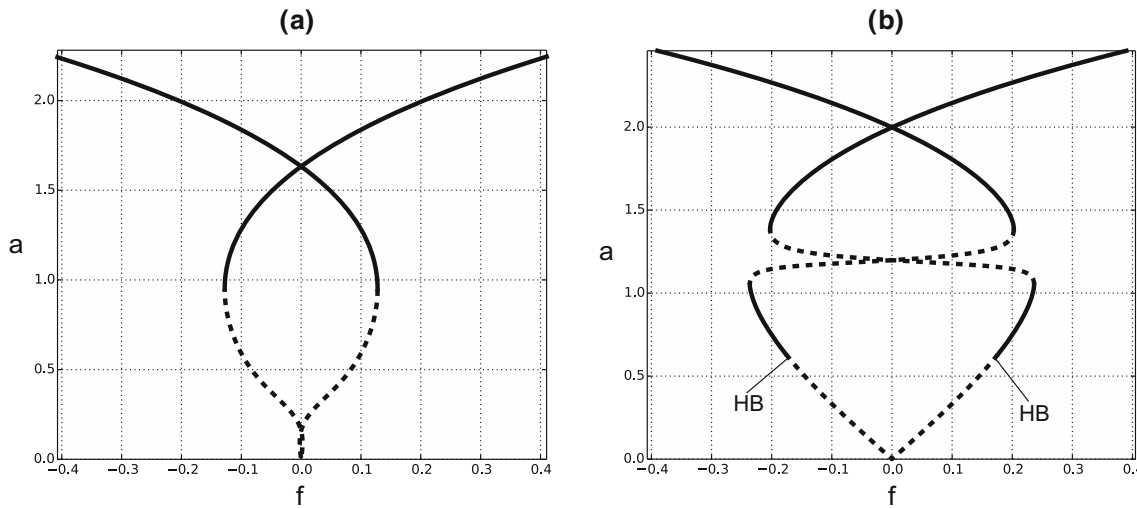


Fig. 12 Bifurcation diagram of amplitude a against external force amplitude f for **a** $\Omega = 1.05$, **b** $\Omega = 1.1$; $g_1 = 0, g_2 = 0$

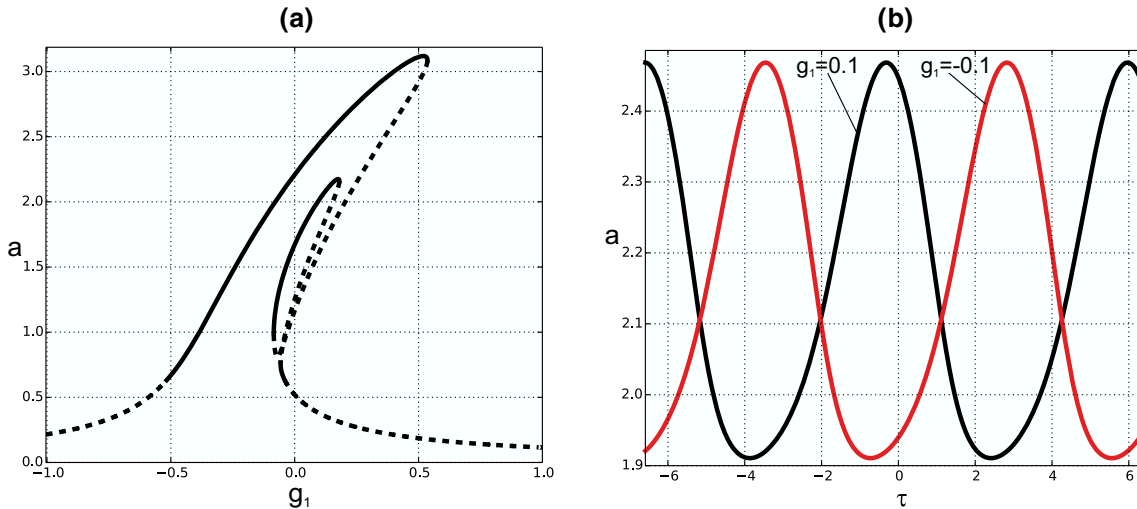


Fig. 13 Bifurcation diagram of amplitude a versus **a** gain g_1 for $\tau = 0$ and **b** versus τ and $g_1 = 0.1$ or $g_1 = -0.1$; $\Omega = 1.1, g_2 = 0, f = 0.15$

detuning parameter, we get the curve remaining the resonance response. Varying time delay τ we may modify amplitude, which repeats periodically depending on the sign of g_1 (Fig. 13b). This is in an accordance with results presented in Chapter 5. The modification of the resonance curve due to displacement feedback is demonstrated in Fig. 14. The gain g_1 mainly moves the curve into left (Fig. 14a) or right (Fig. 14b) direction while time delay τ may eliminate the internal loop and stabilise unstable branches (Fig. 14c, d).

The influence of velocity feedback is more complicated. We demonstrate this assuming $g_1 = 0$. For fixed frequency $\Omega = 1.1$ we get a double loop curve with two Hopf bifurcation points HB_1 and HB_2 leading to instability (Fig. 15). Changing time delay of the velocity feedback we can get different scenarios. Depending on gain value we change amplitude (Fig. 16a) or we can get stable and unstable branches with Hopf bifurcation (Fig. 16b). By a proper selection of the

velocity feedback we can modify frequency locking zones making solutions stable into unstable (see unstable branches in Fig. 17a) or we can stabilise and enlarge the resonance zones (Fig. 17b).

The analytical results are validated by the bifurcation diagram obtained by a direct numerical simulation of the original system (2). Bifurcation diagram (Fig. 18) is in a very good agreement with analytical result presented in Fig. 17a. We can see the stable solution with the internal loop and quasi-periodic oscillations out of the resonance zone.

7 Conclusions

Dynamical properties of MEMS resonator described by Duffing-van der Pol-Mathieu oscillator have been presented

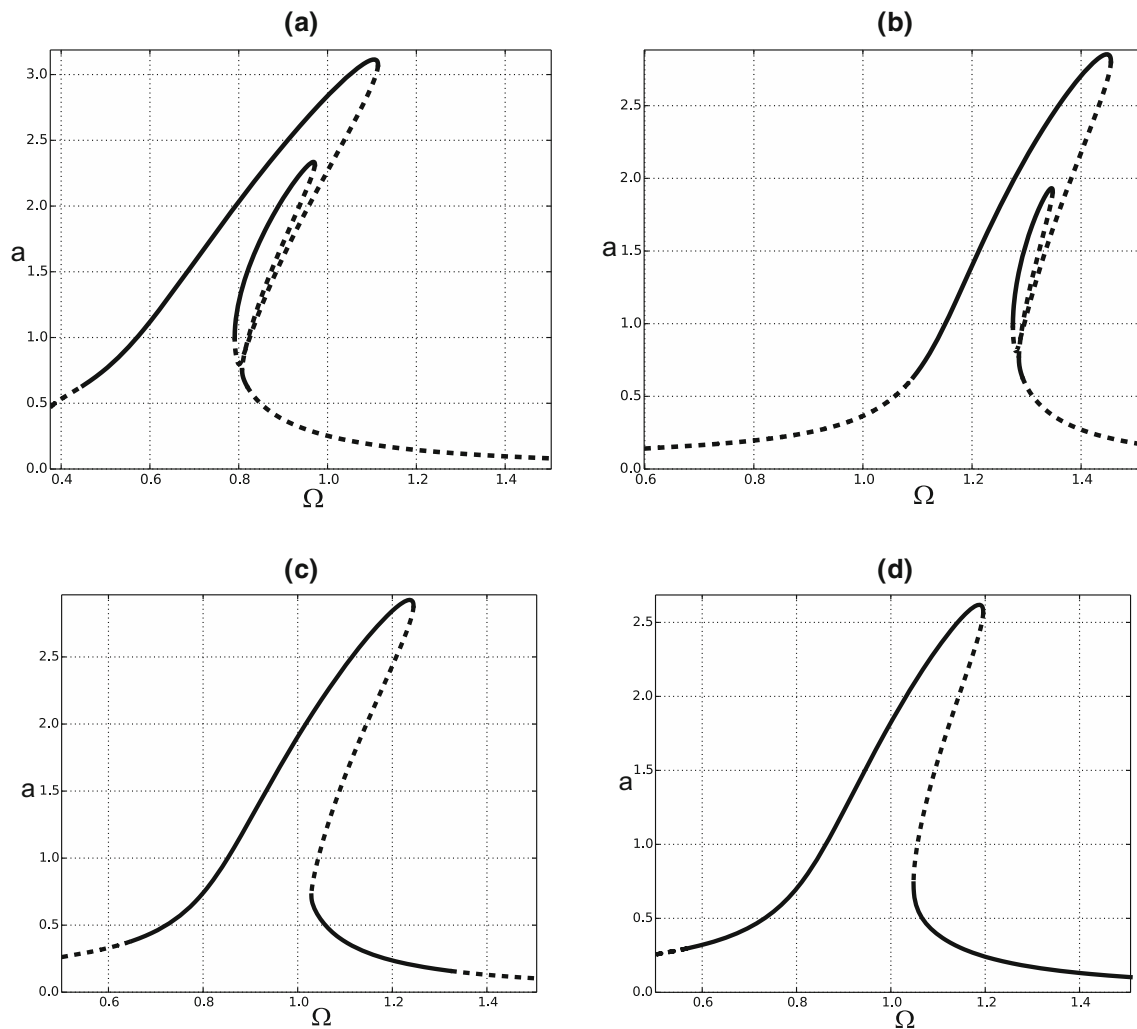


Fig. 14 Influence of gain g_1 on the resonance curves **a** $g_1 = 0.5, \tau = 0$, **b** $g_1 = -0.5, \tau = 0$, **c** $g_1 = 0.1, \tau = 0.1$, **d** $g_1 = 0.1, \tau = 0.5$; $f = 0.15$, $g_2 = 0$

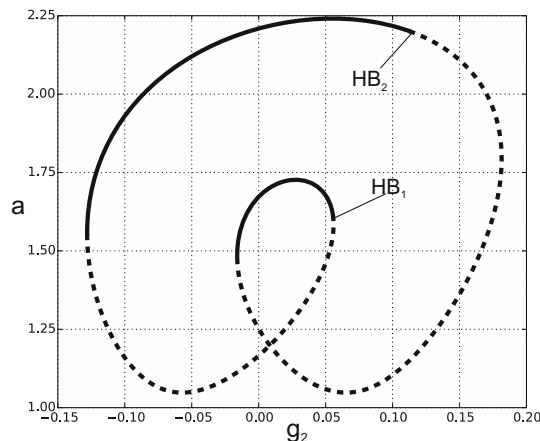


Fig. 15 Bifurcation diagram of amplitude a against gain g_2 for $\tau = 0$, $\Omega = 1.1, g_1 = 0, f = 0.15$

with focus on its periodic oscillations, frequency locking zones and possible control. We show that small external force makes qualitative changes. In the frequency locking zone a

new internal loop occurs with only upper branch stable. The increase of external force diminishes the loop and, above the certain threshold the loop disappears. Furthermore, the increased force stabilises the resonance curve on which one or two Hopf bifurcation points arise. By adding feedback signals we can design feedback control and, depending on the assumed goal, we can stabilise, destabilise or shift the solutions. In some cases we can reduce vibrations to zero.

On the basis of the analytical solutions we can design a model based controller which may adopt to varied parameters. The results show that the gain of displacement feedback g_1 mainly shift the frequency locking zone while its time delay τ may stabilise the solutions. The velocity delayed signal gain g_2 and its time delay modify the solution and stability.

The open problem is the analytical approach to quasi-periodic dynamics, out of the frequency locking zones. This can be done by determining slow-slow flow by using second time the multiple scale method for slow flow. The first attempt

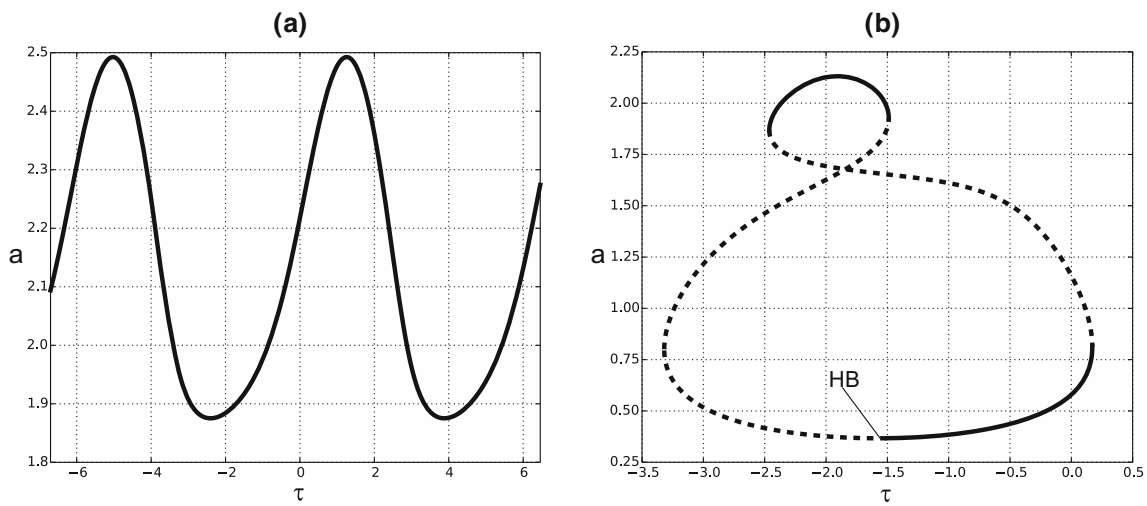


Fig. 16 Bifurcation diagram of amplitude a versus **a** time delay τ for $g_2 = 0.1$ and **b** versus τ and $g_2 = -0.1$; $g_1 = 0$, $f = 0.15$

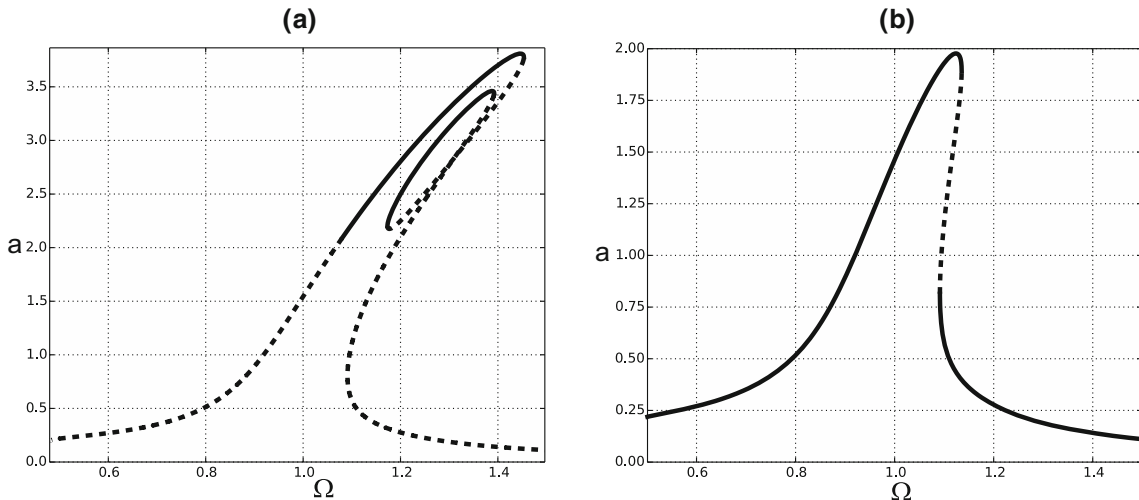


Fig. 17 Influence of gain g_2 on the resonance curves **a** $g_2 = 0.1$, $\tau = 0$, **b** $g_2 = -0.1$, $\tau = 0$; $f = 0.15$, $g_1 = 0$

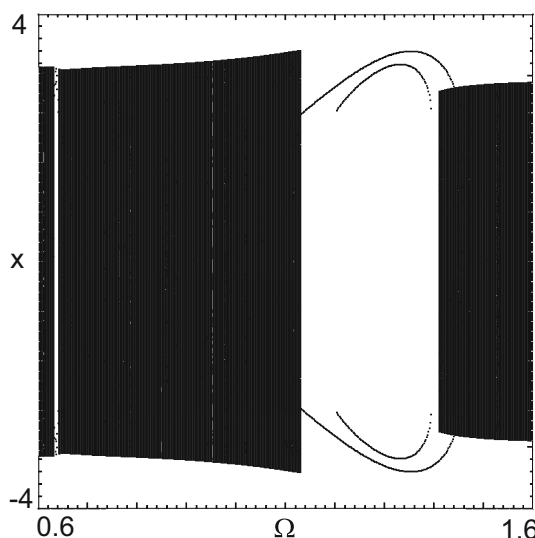


Fig. 18 Bifurcation diagram around the principal resonance for $g_2 = 0.1$, $\tau = 0$, $f = 0.15$, $g_1 = 0$

has been done in [36] and it will be developed in the future to get analytical form for quasi-periodic oscillations of MEMS resonator.

Acknowledgments Author would like to acknowledge the financial support of Structural Funds in the Operational Programme Innovative Economy (IE OP) financed from the European Regional Development Fund Project Modern material technologies in aerospace industry, Nr POIG.01.01.02-00-015/08-00.

Open Access This article is distributed under the terms of the Creative Commons Attribution License which permits any use, distribution, and reproduction in any medium, provided the original author(s) and the source are credited.

Appendix: Second order perturbation analysis—multiple time scale method

The solution of Eq. (2) is assumed in the form of a series of the small parameter ε

$$\begin{aligned} x(t, \varepsilon) &= x_0(T_0, T_1, T_2) + \varepsilon x_1(T_0, T_1, T_2) \\ &\quad + \varepsilon^2 x_2(T_0, T_1, T_2) \\ x_\tau(t, \varepsilon) &= x_{0\tau}(T_0, T_1, T_2) + \varepsilon x_{1\tau}(T_0, T_1, T_2) \\ &\quad + \varepsilon^2 x_{2\tau}(T_0, T_1, T_2) \end{aligned} \quad (18)$$

where $x_j(T_0, T_1, T_2)$, $x_{j\tau}(T_0, T_1, T_2)$ means the solution or delayed solution expressed as a function in the zeroth, first and second order perturbations ($j=0,1,2$), where T_0, T_1, T_2 are respectively the fast and slow time scales. Time is expressed by a series of the small parameter

$$t = T_0 + \varepsilon T_1 + \varepsilon^2 T_2 \quad (19)$$

The introduced time definition results consequently in new definitions of the first and the second time derivatives

$$\begin{aligned} \frac{d}{dt} &= \frac{\partial}{\partial T_0} + \varepsilon \frac{\partial}{\partial T_1} + \varepsilon^2 \frac{\partial}{\partial T_2} = D_0 + \varepsilon D_1 + \varepsilon^2 D_2 \\ \frac{d^2}{dt^2} &= D_0^2 + 2\varepsilon D_0 D_1 + \varepsilon^2 (2D_0 D_2 + D_1^2) \end{aligned} \quad (20)$$

where $D_n^m = \frac{\partial^m}{\partial T_n}$ denotes the m^{th} order partial derivative with respect to the n^{th} time-scale.

Solutions are sought near the principal parametric resonance therefore excitation frequency satisfies the condition (3). Substituting solution (18) into (2), taking into account introduced time scales and the derivatives definition (20), expressing the natural frequency according to (3), after grouping terms with respect to ε , we get a set of differential equations in the successive perturbation orders

$$\varepsilon^0 : D_0^2 x_0 + \Omega^2 x_0 = 0 \quad (21)$$

$$\begin{aligned} \varepsilon^1 : D_0^2 x_1 + \Omega^2 x_1 &= \sigma_1 x_0 - 2D_0 D_1 x_0 + \alpha D_0 x_0 \\ &\quad - \beta x_0^2 D_0 x_0 + \mu x_0 \cos 2\Omega T_0 - \gamma x_0^3 \\ &\quad + g_1 x_{0\tau} + g_2 D_0 x_{0\tau} \end{aligned} \quad (22)$$

$$\begin{aligned} \varepsilon^2 : D_0^2 x_2 + \Omega^2 x_2 &= \sigma_1 x_1 + \alpha (D_0 x_1 + D_1 x_0) \\ &\quad - \beta [x_0^2 (D_0 x_1 + D_1 x_0) + 2x_0 x_1 D_0 x_0] \\ &\quad - 2D_0 D_1 x_1 - 2D_0 D_2 x_0 - D_1^2 x_0 + \mu x_1 \cos 2\Omega T_0 \\ &\quad - 3\gamma x_0^2 x_1 + g_1 x_{1\tau} + g_2 (D_1 x_{0\tau} + D_0 x_{1\tau}) \end{aligned} \quad (23)$$

The solution of Eq. (21) has the form

$$\begin{aligned} x_0(T_0, T_1, T_2) &= A(T_1, T_2) \exp(i\Omega T_0) \\ &\quad + \bar{A}(T_1, T_2) \exp(-i\Omega T_0) \\ x_{0\tau}(T_0, T_1, T_2) &= A(T_1, T_2) \exp(i\Omega T_0 - \tau) \\ &\quad + \bar{A}(T_1, T_2) \exp(-i\Omega T_0 - \tau) \end{aligned} \quad (24)$$

where $i = \sqrt{-1}$ is the imaginary unit, A is the complex amplitude and \bar{A} its complex conjugate and $\tau = \Omega t_d$.

Next, the solution (24) is substituted into (22) and, after grouping the terms in exponential functions, we get

$$\begin{aligned} D_0^2 x_1 + \Omega^2 x_1 &= ST_1 e^{i\Omega T_0} + \left(\frac{1}{2} \mu A \right. \\ &\quad \left. - \gamma A^3 - \beta i \Omega A^3 \right) e^{3i\Omega T_0} + cc \end{aligned} \quad (25)$$

where cc means complex conjugate functions to those written on the right side of Eq. (25) and ST_1 represents secular generating terms. We require vanishing this term therefore $ST_1 = 0$, thus we have

$$\begin{aligned} 2i\Omega D_1 A - \sigma_1 A - i\alpha A\Omega + i\beta\Omega A^2 \bar{A} + 3\gamma A^2 \bar{A} \\ - \frac{1}{2}\mu \bar{A} - (g_1 + g_2 i\Omega) A e^{-i\tau} - \frac{1}{2}f = 0 \end{aligned} \quad (26)$$

Next, rejecting the terms ST_1 we determine the particular solutions of Eq. (25)

$$x_1 = \frac{1}{16\Omega^2} (2\gamma A^3 - \mu A + 2\beta i \Omega A^3) e^{3i\Omega T_0} + cc. \quad (27)$$

Substituting solutions (27) into (23) we get

$$D_0^2 x_2 + \Omega^2 x_2 = NST_2 + ST_2 e^{i\Omega T_0} + cc \quad (28)$$

where NST_2 are nonsecular generating terms and they are not directly reported here, and ST_2 are secular generating terms of the second order which we require vanishing

$$\begin{aligned} D_1^2 A + 2i\Omega D_2 A - \alpha D_1 A + \beta A (2\bar{A} D_1 A + AD_1 \bar{A}) \\ + \frac{1}{2\Omega} \beta \gamma i A^3 \bar{A}^2 - \frac{1}{16\omega} i\beta\mu A (A^2 + \bar{A}^2) \\ + \frac{1}{32\Omega^2} \mu^2 A + \frac{3}{8\Omega^2} \gamma^2 A^3 \bar{A}^2 - \frac{1}{8} \beta^2 A^3 \bar{A}^2 \\ - \frac{1}{16} \gamma \mu A (A^2 + 3\bar{A}^2) - g_2 D_1 A e^{-i\tau} = 0 \end{aligned} \quad (29)$$

Taking into account the particular solutions (24) and (27), expressing the complex amplitudes in the polar form:

$$A = \frac{1}{2}ae^{i\phi} \quad (30)$$

then using expansion (18), and after transformation to the trigonometric form, we obtain approximate solutions in the zeroth and the first order approximation (4).

Applying the so called reconstitution method [35], on the basis of Eqs. (26) and (29) we reconstruct the ordinary differential equation for a modulation of the complex amplitudes A . Expressing complex amplitude A in the polar form (30) and separating the real and imaginary parts, we get the modulation Eqs. (5) for amplitude a and phase ϕ . These are so called ‘slow flow’ equations.

References

1. Wong AC, Nguyen CTC, Ding H, RF MEMS for wireless applications (1999) In: IEEE international solid-state circuits conference, vol 448. p 78
2. Bruland KJ, Rugar D, Zuger O, Hoen S, Sidles JA, Garbini JL, Yannoni CS (1995) Magnetic resonance force microscopy. *Rev Mod Phys* 67:249
3. Sarid D (1994) Scanning force microscopy with applications to electric magnetic and atomic forces. Oxford University Press, New York
4. Pandey M, Aubin K, Zalalutdinov M, Zehnder A, Rand R (2006) Analysis of frequency locking optically driven MEMS resonators. *IEEE J Microelectromech Syst* 15:1546–1554
5. Pandey M, Rand R, Zehnder A (2007) Perturbation analysis of entrainment in a micromechanical limit cycle oscillator. *Commun Nonlinear Sci Numer Simul* 12:1291–1301
6. Pandey M, Rand R, Zehnder A (2008) Frequency locking in a forced Mathieu–van der Pol–Duffing system. *Nonlinear Dyn* 54:3–12
7. Blocher DB, Zehnder AT, Rand RH (2013) Entrainment of micro-mechanical limit cycle oscillators in the presence of frequency instability. *IEEE/ASME J Micromech Syst* 22(4):835–845
8. Aubin K, Zalalutdinov M, Alan T, Reichenbach R, Rand R, Zehnder A, Paria J, Craighead H (2004) Limit cycle oscillations in CW laser driven NEMS. *IEEE/ASME J Micromech Syst* 13:1018–1026
9. Aubin K, Zalalutdinov M, Reichenbach RB, RHuston B, Zehnder AT, Paria JM, Craighead HG (2003) Laser annealing for high-q MEMS resonators. *Proc SPIE* 5116:531–535
10. Blocher D, Rand RH, Zehnder AT (2013) Multiple limit cycles in laser interference transduced resonators. *Int J Non-Linear Mech* 52:119–126
11. Blocher D, Rand RH, Zehnder AT (2013) Analysis of laser power threshold for self oscillation in thermo-optically excited doubly supported MEMS beams. *Int J Non-Linear Mech* 57:10–15
12. Szabelski K, Warminski J (1995) The parametric self-excited nonlinear system vibrations analysis with the inertial excitation. *Int J Non-Linear Mech* 30(2):179–189
13. Szabelski K, Warminski J (1995) The self-excited system vibrations with the parametric and external excitations. *J Sound Vib* 187(4):595–607
14. Warminski J (2001) Synchronisation effects and chaos in the van der Pol–Mathieu oscillator. *J Theor Appl Mech* 39(4):861–884
15. Szabelski K, Warminski J (1997) Vibrations of a non-linear self-excited system with two degrees of freedom under external and parametric excitation. *Int J Nonlinear Dyn* 14:23–36
16. Warminski J (2010) Nonlinear normal modes of a self-excited system driven by parametric and external excitations. *Nonlinear Dyn* 61:677–689
17. Belhaq M, Houssni M (1999) Quasi-periodic oscillations, chaos and suppression of chaos in a nonlinear oscillator driven by parametric and external excitations. *Nonlinear Dyn* 18:1–24
18. Belhaq M, Fahsi A (2009) Hysteresis suppression for primary and subharmonic 3:1 resonances using fast excitation. *Nonlinear Dyn* 57:275–287
19. Fahsi A, Belhaq M (2009) Hysteresis suppression and synchronization near 3:1 subharmonic resonance. *Chaos Solitons Fractals* 42:1031–1036
20. Verhulst F (2005) Quenching of self-excited vibrations. *J Eng Math* 53:349–358
21. Abadi (2003) Nonlinear dynamics of self-excitation in autoparametric systems. University of Utrecht, Netherlands
22. Pust L, Tondl A (2008) System with a non-linear negative self-excitation. *Int J Non-Linear Mech* 43:497–503
23. Tondl A, Ecker H (1999) Cancelling of self-excited vibrations by means of parametric excitation. In: Proceedings of the ASME design engineering technical conferences, 12–15 September, Las Vegas, Nevada, USA
24. Dohnal F (2008) Damping by parametric stiffness excitation: resonance and anti-resonance. *J Vib Control* 14(5):669–688
25. Tondl A, Nabergoj R (2004) The effect of parametric excitation on a self-excited three-mass system. *Int J Non-Linear Mech* 39:821–832
26. Rand R, Barcilon A, Morrison T (2005) Parametric resonance of Hopf bifurcation. *Nonlinear Dyn* 39:411–421
27. Rand R, Morrison T (2005) 2:1:1 Resonance in the quasi-periodic Mathieu equation. *Nonlinear Dyn* 40:195–203
28. Luongo A, Zulli D (2011) Parametric, external and self-excitation of a tower under turbulent wind flow. *J Sound Vib* 330:3057–3069
29. Zulli D, Luongo A (2012) Bifurcation and stability of a two-tower system under wind-induced parametric, external and self-excitation. *J Sound Vib* 331:365–383
30. Warminski J, Warminska A (2013) Parametric resonance of a self-excited system under external force and time delay influence. In: Proceedings of the ASME 2013 international design engineering technical conferences and computers and information in engineering conference, IDETC/CIE 2013, 4–7 August 2013, Portland, Oregon, USA, DETC2013-12564
31. Hu H, Dowell EH, Virgin LN (1998) Resonances of a harmonically forced Duffing oscillator with time delay state feedback. *Nonlinear Dyn* 15:311–327
32. Rusinek R, Weremczuk A, Kecik K, Warminski J (2014) Dynamics of a time delayed Duffing oscillator. *Int J Non-Linear Mech* 65:98–116
33. Morrison TM, Rand RH (2007) 2:1 Resonance in the delayed nonlinear Mathieu equation. *Nonlinear Dyn* 50:341–352
34. Macaari A (2008) Vibration amplitude control for a van der Pol–Duffing oscillator with time delay. *J Sound Vib* 317:20–29
35. Nayfeh AH (1985) Problems in perturbations. John Wiley & Sons, Inc
36. Warminski J, Warminska A (2014) Hopf bifurcations, quasi-periodic oscillations and frequency locking zones in a self-excited system driven by parametric and external excitations. In: Proceedings of the ASME 2014 international design engineering technical conferences and computers and information in engineering conference, IDETC/CIE 2014, 17–20 August 2014, Buffalo, NY, USA, DETC2014-34079
37. Doedel EJ, Champneys AR, Fairgrieve TF, Kuznetsov YA, Sandstede B, Wang X (1998) Auto 97: continuation and bifurcation software for ordinary differential equations. <http://indy.cs.concordia.ca/auto>